



ORIGINAL ARTICLE

Corrosion inhibition performance of different bark extracts on aluminium in alkaline solution



Namrata Chaubey^a, Savita^a, Vinod Kumar Singh^a, M.A. Quraishi^{b,*}

^a Department of Chemistry, Udai Pratap Autonomous College, Varanasi 221002, India

^b Department of Chemistry, Indian Institute of Technology (Banaras Hindu University), Varanasi 221005, India

Received 2 June 2015; revised 14 December 2015; accepted 17 December 2015

Available online 25 January 2016

KEYWORDS

Aluminium Alloy;
EIS;
Corrosion inhibition;
SEM;
AFM

Abstract The present work shows the effect of stem bark extracts of three trees namely *Moringa oleifera* (MO), *Terminalia arjuna* (TA) and *Mangifera indica* (MI) on the corrosion behaviour of Aluminium Alloy (AA) in 1 M NaOH. The inhibition performance was studied by using gravimetric, potentiodynamic polarization and electrochemical impedance spectroscopy (EIS) measurements. Among these extracts, MO exhibited the maximum inhibition efficiency η (%) of 85.3% at 0.6 g/L at 303 K. Polarization measurement showed that all the examined extracts are of mixed-type inhibitors. Langmuir's adsorption isotherm was found to be best fit. Morphology of the surface was examined by scanning electron microscopy (SEM) and atomic force microscopy (AFM) which confirmed the existence of a protective film of inhibitor molecule on AA surface.

© 2016 University of Bahrain. Publishing services by Elsevier B.V. This is an open access article under the CC BY-NC-ND license (<http://creativecommons.org/licenses/by-nc-nd/4.0/>).

1. Introduction

Aluminium and its alloys are finding wide applications in various industries such as automotive, aerospace, construction and electrical power generation due to high energy density (8.1 kWh kg⁻¹) and an electrode potential of 2.35 V vs. simple hydrogen electrode (SHE) in alkaline medium. Alkaline solution is most corrosive in nature for aluminium than the other corrosive media. Therefore, it is desirable to study the corrosion and protection of aluminium in alkaline medium. The corrosion resistance of aluminium depends on the presence of natural surface oxide film and stability. It is

reported that due to the presence of OH⁻ ion protective oxide film dissolves in alkaline solution and negative potential develops on the aluminium surface (Abiola and Otaigbe, 2008). In the development of the aluminium anode for the aluminium/air battery, the corrosion behaviour of pure aluminium and its alloys has been extensively studied in aqueous alkaline solutions, that's why self-corrosion can cause not only a lower utilization efficiency of aluminium, but also possible battery explosion as a result of hydrogen build up (Oguzie, 2007). Plenty of organic and inorganic compounds have been used by various researchers as corrosion inhibitors to protect the dissolution of this oxide film (Abdel-Gaber et al., 2008) and thus reducing the rate of metal loss in alkaline medium. Most of the compounds are synthetic chemicals which are expensive and hazardous to the environment. Thus it is desirable to choose a very cheap and environmentally safe inhibitor to diminish the self-corrosion rate of aluminium in alkaline solution.

* Corresponding author. Tel.: +91 9307025126; fax: +91 542 2368428.

E-mail addresses: maquraishi.apc@itbhu.ac.in, maquraishi@rediffmail.com (M.A. Quraishi).

Peer review under responsibility of University of Bahrain.

<http://dx.doi.org/10.1016/j.jaubas.2015.12.003>

1815-3852 © 2016 University of Bahrain. Publishing services by Elsevier B.V.

This is an open access article under the CC BY-NC-ND license (<http://creativecommons.org/licenses/by-nc-nd/4.0/>).

For this purpose, the natural products of plant origin are a better choice because they are environmentally benign and contain incredibly rich source of naturally synthesized organic compounds in which most are known to have inhibitive action that can be extracted using simpler techniques with low cost. There are few studies available on the use of plant extract as corrosion inhibitor for aluminium in alkaline medium (Abiola and Otaigbe, 2009; Abdel-Gaber et al., 2008; Chaubey et al., 2015). In the present work, we have selected the aqueous extract of the bark of MO, TA and MI for the corrosion inhibition study on AA in 1 M NaOH solution by using gravimetric, potentiodynamic polarization and electrochemical impedance spectroscopy measurement respectively. The experimental results were supported by SEM and AFM investigations.

2. Materials and methods

2.1. Specimen and test solution

Corrosion tests were performed on AA specimens of following composition (wt.%): Si = 0.77, Fe = 0.93, Cu = 0.02, Mn = 0.11, Mg = 0.01, Zn = 0.01, Cr = 0.05, Ti = 0.02, V = 0.01, Ga = 0.01 and remainder Al. The aggressive solution of 1 M NaOH is prepared by dissolving 40 g of sodium hydroxide pellets in 1000 ml of double distilled water.

2.2. Preparation of bark extracts solution

MO, TA and MI tree barks were collected and dried in shade. 5 g of dried bark powder was taken in 500 ml of NaOH in a round bottom flask and refluxed for 3 h. The solution was allowed to stand for some time and then filtered. The volume of the filtrate solution was maintained up to 100 ml, which was used as stock solution of inhibitors. After that, the residue of all barks was dried and weighed and taken in different concentrations for the experiment.

2.3. Gravimetric measurement

The dimension of AA coupon used in the gravimetric study is $2.5 \times 2.0 \times 0.043$ cm. Silicon carbide papers with grade 600, 800 and 1000 were used for abrasion of AA coupons and finally degreased with acetone and dried at room temperature. The gravimetric measurement was carried out in the temperature range of 303–333 K, with an immersion period of 3 h. The corrosion rate (C_R) and inhibition efficiency ($\eta\%$) was calculated using the following equations :

$$C_R = \frac{K \times W}{A \times T \times D} \quad (1)$$

$$\eta\% = \frac{w_0 - w_i}{w_0} \times 100 \quad (2)$$

where K is constant (87.6×10^4), T is the exposure time in hours (h), A is the area of a coupon in cm^2 , W is the weight loss in gram (g), D is the density of AA in g/cm^3 , w_0 and w_i are the weight loss in the absence and presence of inhibitors, respectively.

2.4. Electrochemical experiment

The dimension of AA coupons used for the electrochemical study is $7.0 \times 1.0 \times 0.043$ cm. Electrochemical measurement was carried out by using Gamry Potentiostat/Galvanostat (Model 300) at 303 K. Three electrode cell assemblies were used for this measurement, in which AA, calomel and platinum foil were used as working, reference and counter electrodes respectively. For data fitting Echem Analyst (version 5.0 software) packages were used. EIS measurements were performed in the frequency range 10^6 – 10^{-2} Hz using AC signals of amplitude 10 mV peak to peak at open circuit potential.

Potentiodynamic polarization curves were obtained by changing the electrode potential automatically from -0.25 V to $+0.25$ V vs. OCP at a scan rate of 1 mV/s. The anodic and cathodic curves of the linear Tafel plots were extrapolated to obtain corrosion current densities (i_{corr}). All the experiments were measured after immersion of AA for 15 min in 1 M NaOH in the absence and presence of inhibitors.

2.5. Surface analysis

AA coupons of size $2 \times 2.5 \times 0.046$ cm were immersed in 1 M NaOH in the absence and presence of inhibitor for 3 h at 303 K. The inhibited system contains optimum concentration (0.6 g/L) of MO, TA and MI barks. FEI Quanta 200F microscope model was used for SEM at an accelerating voltage of 5000 V and 5KX magnification. The AFM was performed using NT-MDT multimode, Russia, controlled by solver scanning probe microscope controller.

3. Results and discussion

3.1. Gravimetric measurements

3.1.1. Effect of inhibitor concentration

The inhibition efficiencies with different concentrations of barks are compiled in Fig. 1. It can be seen from Fig. 1 that gradually increased inhibitor concentration increases the percentage inhibition efficiency ($\eta\%$). The inhibitive action of the inhibitor is due mainly to the presence of Hetero atoms such as oxygen, nitrogen and aromatic rings with π -bonds in

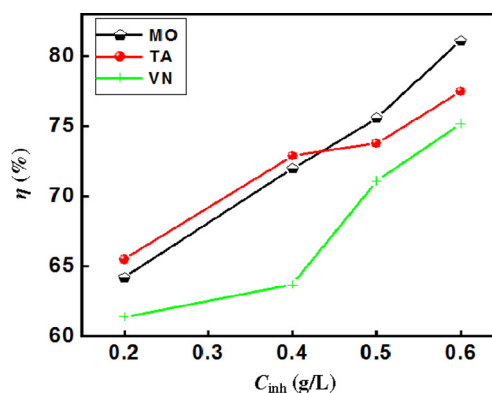


Figure 1 Variation of inhibition efficiencies ($\eta\%$) with concentration of bark extracts for AA in 1 M NaOH.

their constituents, which creates a protective film on it (Abood, 2011). Very good inhibition efficiency ($\eta\%$) was obtained (85.3% for MO) at 0.6 g/L. The order of inhibition efficiency ($\eta\%$) are as follows:

MO > TA > MI

The better inhibition efficiencies observed by these extracts can be explained by the larger coverage of metal surface by inhibitor molecules (Yadav and Quraishi, 2012).

3.1.2. Effect of temperature

The influence of temperature on inhibition efficiency and corrosion rate values was studied by weight loss experiment at different temperatures (303–333 K) in the absence and presence of 0.6 g/L bark extracts in 1 M NaOH. It can be seen in Table 1, as the temperature increases, there is increase in C_R and decrease in $\eta\%$ values respectively. This occurs due to desorption of inhibitor molecules.

The apparent activation energy (E_a) can be calculated by using Arrhenius equation

$$C_R = A \exp\left(\frac{-E_a}{RT}\right) \quad (3)$$

where E_a is the apparent activation energy, R is the gas constant and A is the Arrhenius pre-exponential factor.

A straight line was obtained by plotting a graph between $\log C_R$ versus $1/T$ as shown in Fig. 2, with a slope value of $E_a/2.303 R$. It was observed that the value of E_a for uninhibited system is 33.6 kJ/mol which is much lower than the values observed for MO (60.5 kJ/mol), TA (50.1 kJ/mol) and MI (43.65 kJ/mol). Higher values of E_a for inhibited system are explained by the formation of a physical barrier to charge and mass transfer created by the adsorbed inhibitor molecules (Chaubey et al., 2015). The above E_a values in the presence of inhibitors are larger than in other absence, but lower than 80 kJ mol⁻¹ which is the threshold value for

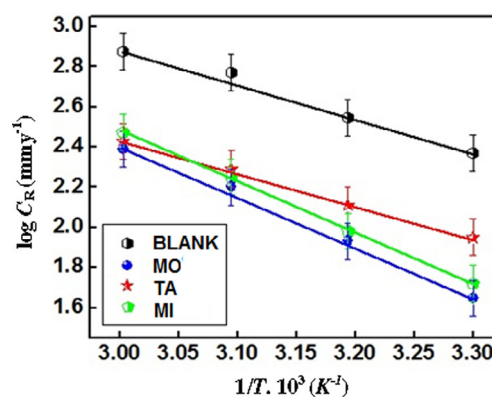


Figure 2 Arrhenius plot for AA corrosion rates (C_R) in 1 M NaOH without and with optimum concentration (0.6 g/L) of inhibitors.

chemical adsorption. This suggests physical adsorption of inhibitor molecules.

3.1.3. Adsorption isotherm

To find out the mechanism of corrosion inhibition by the interaction of the inhibitor molecules with the active site of the AA, adsorption isotherm experiment was performed. Langmuir adsorption isotherm was found to be best fit among various adsorption isotherms and it is given by the relation (Bammou et al., 2014):

$$\frac{C_{inh}}{\theta} = \frac{1}{K_{ads}} + C_{inh} \quad (4)$$

where K_{ads} is the adsorption equilibrium constant, C_{inh} is inhibitor concentration. A straight line was obtained by plotting between C_{inh}/θ and C_{inh} , supporting that adsorption of inhibitors follows Langmuir adsorption isotherm.

The linear regression and slope values observed for MO, TA and MI are 0.993 and 1.086, 0.997 and 1.181, 0.987 and 1.187 respectively. It can be clearly seen in Fig. 3 that for all the inhibitors, slope value is 1 and linear correlation coefficients (r) is close to 1, suggesting the adsorption of inhibitor molecule on aluminium surface obeys the Langmuir adsorption isotherm.

Table 1 Parameters obtained from gravimetric test for AA in 1 M NaOH containing 0.6 g/L concentrations of the inhibitors at different temperatures.

Inhibitors	Temperature (K)	C_R (mmy ⁻¹)	η (%)
Blank	303	351.0	–
	313	528.1	–
	323	885.6	–
	333	1127	–
MO	303	34.60	85.3
	313	85.40	75.9
	323	166.5	72.0
	333	264.9	65.0
TA	303	52.91	77.5
	313	96.23	72.8
	323	178.4	70.9
	333	298.4	60.5
MI	303	58.45	75.2
	313	105.8	70.1
	323	195.7	67.1
	333	268.2	59.4

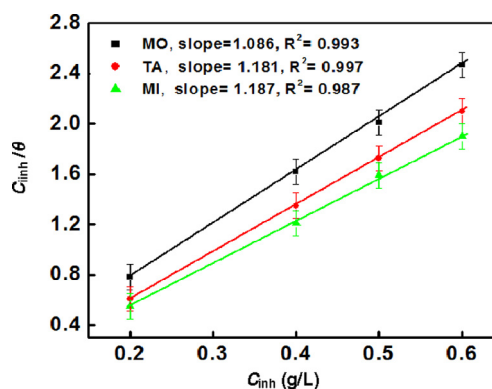


Figure 3 Langmuir's isotherm plots for adsorption of inhibitors on aluminium in 1 M NaOH.

3.2. Electrochemical measurement

3.2.1. Potentiodynamic polarization

Potentiodynamic polarization curves for aluminium metal in 1 M NaOH at optimum concentration (0.6 g/L) of bark extracts are displayed in Fig. 4. Electrochemical parameters associated with polarization measurements such as anodic and cathodic Tafel constants (β_a and β_c), corrosion potential (E_{corr}) and corrosion current density (i_{corr}) were calculated and given in Table 2. It can be observed from Fig. 4 that in the presence of inhibitors both the anodic and cathodic curves are shifting towards lower current density. Also as inhibitors are added i_{corr} values are going to decreased (Table 2), which reveals that inhibitor molecules are adsorbed on the AA surface.

The $\eta\%$ using i_{corr} value was calculated by the following equation (Anejjar et al., 2014):

$$\eta\% = \frac{i_0 - i}{i_0} \times 100 \quad (5)$$

where i_0 and i are the corrosion current densities in the absence and presence of inhibitors, respectively. If the value of E_{corr} shifts beyond 85 mV, a chemical compound can be designated as an anodic or a cathodic type inhibitor (Ansari and Quraishi, 2015). In our study, the maximum displacement is about 32 mV which is less than 85 mV, suggesting that the studied inhibitors are of mixed type. It is evident from Table 2 that with increasing extract concentration, values of b_c and b_a decreases. After comparing the literature (Singh et al., 2012) it was observed that the decrease in b_c may be attributed to the adsorption of an inhibitor molecule on the metal surface and hindered the alkali attack, therefore, did not change the hydrogen evolution reaction mechanism. In the anodic case, the decrease in b_a might be attributed to the modification of anodic dissolution process because of adsorption of the inhibitor molecule on the active sites. The cathodic and anodic slopes shifted to the lower current density, as compared to the blank thus, the inhibition efficiency ($\eta\%$) increased with increasing the extract concentration and reaching a maximum value of 85.7% for MO at 0.6 g L⁻¹.

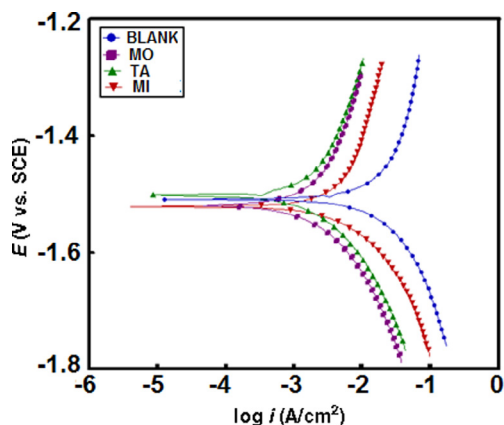


Figure 4 Tafel curves for aluminium in 1 M NaOH in the absence and presence of optimum concentration (0.6 g/L) of inhibitors at 303 K.

Table 2 Potentiodynamic polarization parameters for AA in 1 M NaOH in the absence and presence of optimum concentration of inhibitors at 300 K.

Inhibitors	Tafel polarization				
	I_{corr} (mA cm ⁻²)	E_{corr} (mV/SCE)	β_a (mV/dec)	β_c (mV/dec)	η (%)
Blank	96.3	-1508	1001	504	-
MO	13.9	-1520	806	100	86.5
TA	18.8	-1500	780	153	81.2
MI	20.4	-1540	673	166	79.1

3.2.2. Electrochemical impedance spectroscopy

The corrosion behaviour of AA specimen was also investigated by EIS technique at optimum concentration of inhibitors and given in Fig. 5. As can be seen from Fig. 5, the impedance diagram is explained by the semicircles, suggesting that the corrosion process occurs mainly through charge transfer (Prabhu and Rao, 2014). With increasing the inhibitor concentrations, a noticeable change in impedance modulus of AA in 1 M NaOH solution occurs by increasing the diameter but there is no change occurring in corrosion mechanism. It is proved by similar shape of impedance modulus in the absence and presence of inhibitors. Three loops are manifested in Fig. 5: a large capacitive loop at higher frequency (HF) region, a second capacitive loop at lower frequency (LF) region separated by an inductive loop of intermediate frequencies (IF).

For calculation of impedance data an equivalent circuit depicted in Fig. 6 was used. This equivalent circuit contains solution resistance (R_s), charge transfer resistance (R_{ct}) and inductive elements (R_L and L). In the presence of inhibitors, the appearance of L is explained by the fact that aluminium is still going to dissolve via charge transfer process on the adsorbed inhibitor aluminium surface. In this circuit another constant phase element (CPE_2) is present which is placed in parallel to charge transfer resistance element R_{ct2} . The measurement of charge-transfer resistance corresponds to the $\text{Al}^+ - \text{Al}^{3+}$ reaction is defined by R_{ct2} . To compensate for non-homogeneity in the system, the CPE is used in this model which is defined by two values, Q and n . The impedance of CPE is represented by:

$$Z_{CPE} = \frac{1}{Q(j\omega)^n} \quad (6)$$

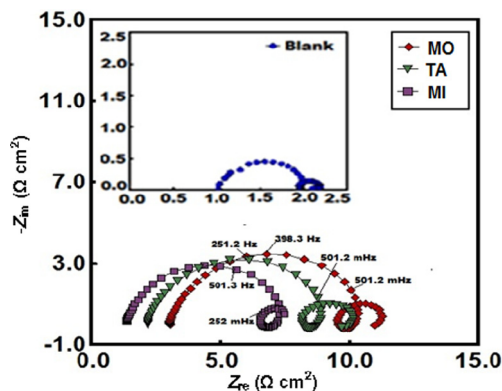


Figure 5 Nyquist plots of AA in 1 M NaOH without and with optimum concentration (0.6 g/L) of inhibitors at 303 K.

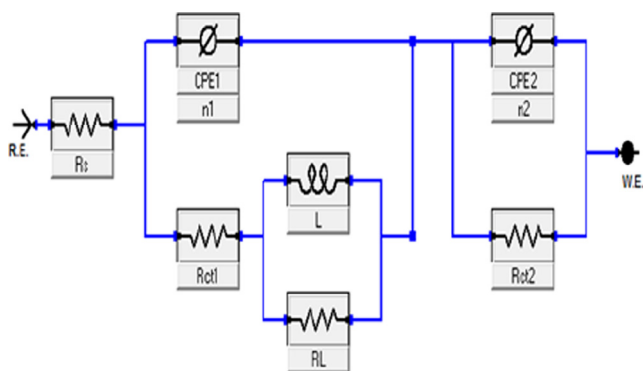


Figure 6 Electrical equivalent circuit used for the analysis of impedance spectra.

where Q denotes the proportionality constant comparable to capacitance, j is the imaginary unit and ω is the angular frequency ($\omega = 2\pi f$, f is the frequency at maximum in Hz), n is the phase shift which is related to degree of surface non-homogeneity. The double layer capacitance (C_{dl}) is deduced from the following equation.

$$C_{dl} = Q \times (2\pi f_{max})^{n-1} \quad (7)$$

From the Table 3, it can be observed that the value of double layer capacitance (C_{dl}) decreases in the presence of inhibitors, due to adsorption of inhibitor molecules over the AA surface. Analysis of Table 3 reveals the presence of inhibitors increase the value of R_{ct} than those of the inhibitor free system. The increase in R_{ct} values for the inhibited system is attributed to the decrease in the active surface necessary for the corrosion reaction and it also may be imputed with a slower corrosion rate. The inhibition efficiency associated with charge transfer resistance value is calculated by the following equation:

$$\eta\% = \frac{R_{CT(i)} - R_{CT(0)}}{R_{CT(i)}} \times 100 \quad (8)$$

where $R_{ct(i)}$ and $R_{ct(0)}$ are the charge transfer resistance values with and without inhibitor, respectively.

Bode impedance and phase angle plots are shown in Fig. 7. It is well known that the value of S and α° for an ideal capacitor should be -1 and -90° respectively. However the maximum slope value and maximum phase angle observed in the present study are -0.79 and 69° respectively. These deviations at intermediate frequencies are known to be the deviation from the ideal capacitive behaviour. The approaching of S and α° value towards ideal capacitor reveals the adsorption of inhibitor molecules over the AA surface.

3.2.3. Surface analysis

SEM images of AA surface exposed to 1 M NaOH without and with 0.6 g/L bark extract for 3 h are given in Fig. 8a–d. Fig. 8a is the micrograph of the AA surface in the absence of inhibitor

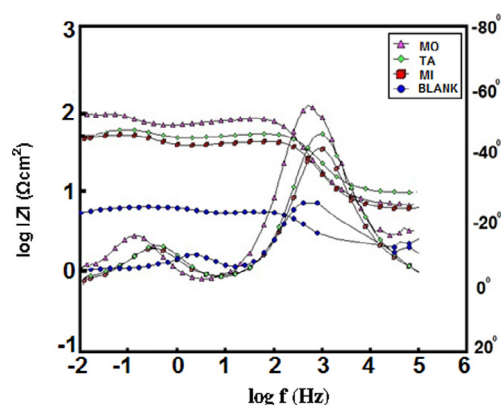


Figure 7 Bode ($\log f$ vs. $\log |Z|$) and phase angle ($\log f$ vs. α) plots of impedance spectra for aluminium in 1 M NaOH in the absence and presence of optimum concentration of inhibitors at 303 K.

and its inspection reveals that there are clear pits and cavities are observed with roughness due to strong damage by the attack of NaOH. Fig. 8b–d are the micrographs in the presence of inhibitors. The close observation of these micrographs proved that there is less damage to the Aluminium surface, which is achieved due to adsorption of inhibitor molecules.

3.2.4. Atomic force microscope

Atomic force microscopy is a powerful technique for gathering of roughness statistics from a variety of surfaces. AFM is becoming an accepted method of roughness investigation (Hakeem et al., 2014). The three-dimensional AFM images of the AA surface in the absence and presence of inhibitors are shown in Fig. 9a–d. Fig. 9a displays the image of the AA coupon after immersing in uninhibited 1 M NaOH solution for 3 h as strongly damaged. The maximum height scale of the AA surface in corrosive solution was 800 nm. After adding inhibitors the surface appears more flat, homogeneous and uniform (Fig. 9b–d). The maximum height scales of the surface were 150 nm, 180 nm and 250 nm for MO, TA and MI respectively. These results suggested that the bark extract inhibitor shows an appreciable resistance to corrosion.

3.3. Inhibition study of constituents

The aqueous extract of barks contains various phytochemical components such as 4-(alpha-l-rhamnopyranosyloxy)-benzylglucosinolate in MO (Mishra et al., 2011). Tannin, saponin, and flavonoids are in TA. Xanthone C-glucoside mangiferin as a major component in MI (Chidozie and Adoga, 2014). The molecular structure of major active constituents is given in Table 4. These constituents contain π -bonds, nitrogen and oxygen atoms in their molecular structures as active centres for adsorption.

Table 3 Electrochemical impedance parameters for AA in 1 M NaOH in the absence and presence of optimum concentration of inhibitors at 300 K.

Inhibitors	R_s (Ω)	Q_1 ($S\Omega^{-1} cm^{-2}$)	n	$(R_{ct})_1$ (Ωcm^2)	L (Hcm ²)	R_L (Ωcm^2)	Q_2 ($S\Omega^{-1} cm^{-2}$)	$(R_{ct})_2$ (Ωcm^2)	C_{dl} ($\mu F cm^{-2}$)	η (%)
Blank	1.023	500×10^{-6}	0.975	0.849	0.221	0.121	39.8×10^{-6}	0.188	413.8	–
MO	1.430	94.6×10^{-6}	0.991	6.723	0.145	2.268	77.2×10^{-6}	1.402	73.97	85.4
TA	2.323	141.9×10^{-6}	0.989	4.112	0.166	3.434	62.1×10^{-6}	1.039	78.05	79.1
MI	1.423	166.1×10^{-6}	0.982	2.934	0.218	2.340	48.8×10^{-6}	1.022	95.56	72.0

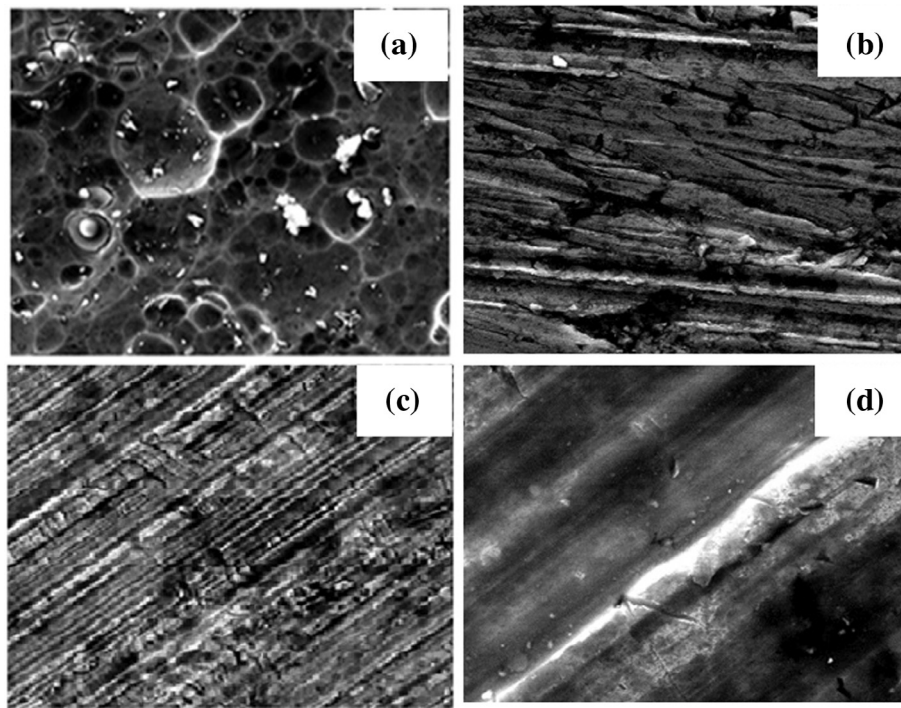


Figure 8 SEM micrographs of (a) uninhibited and (b) inhibited AA sample containing 0.6 g/L of MO (c) TA (d) MI in 1 M NaOH.

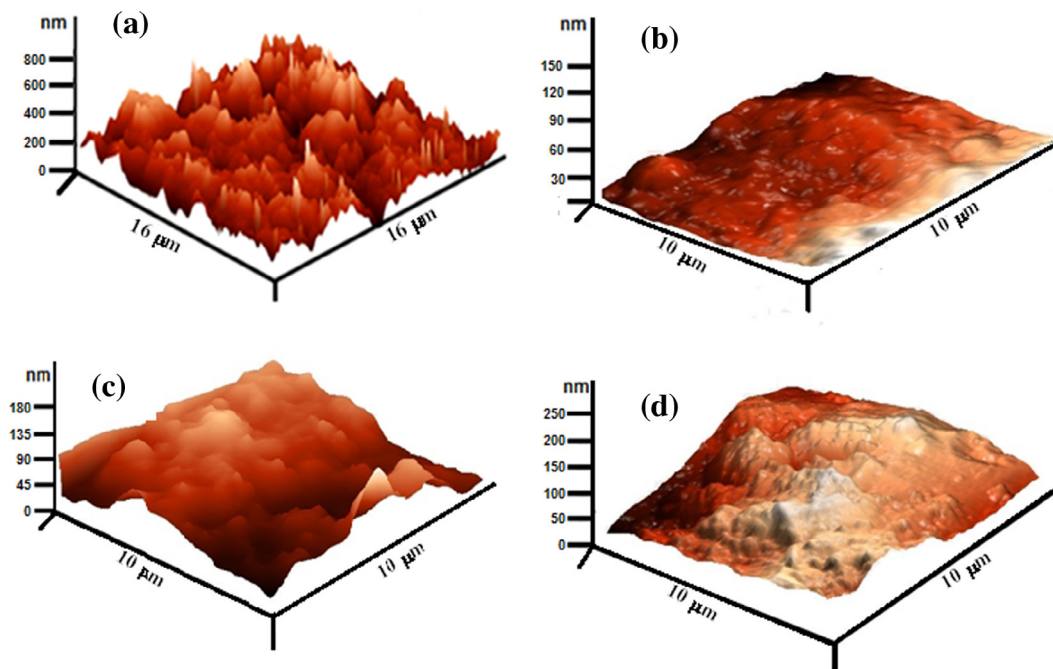
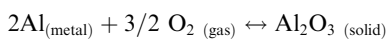


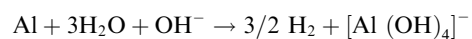
Figure 9 AFM spectra of aluminium specimens (a) uninhibited and (b) MO (c) TA (d) MI in 1 M NaOH.

It can be suggested that aluminium combines with ambient oxygen for the formation of an oxide layer film



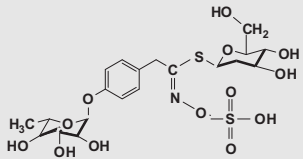
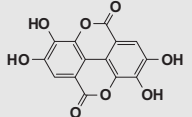
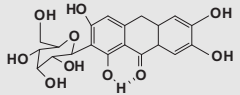
The oxide film formed acts as a static barrier that isolates the metal from the solution. However, alkaline solutions are

known to destroy its property. The aluminium dissolution reaction in alkaline medium is due to the following reaction:



The soluble complex ion formed leads to the dissolution of the metal. Adsorption of the inhibitor at the AA surface occurs by replacing water molecules. Basically adsorption of inhibitors

Table 4 Molecular structure of major constituents present in extracts.

Inhibitors	Major constituents	Molecular structure	Refs.
MO	4-(alpha-l-rhamnopyranosyloxy)-benzylglucosinolate		Mishra et al. (2011)
TA	Ellagic acid		Harika et al. (2013)
MI	Mangiferin		Chidozie and Adoga (2014)

occurs due to the presence of heteroatoms, –OH groups and pi bonds, which creates a protective film on it. This restricts the diffusion of ions to or from the metal surface and hence retards the overall corrosion process. The high inhibition performance by MO bark extract is due to large size of constituent's molecule which covers wide areas on the AA surface (Quraishi et al., 2010).

4. Conclusion

Among studied bark extracts, MO is found to give effective protection for aluminium in NaOH solution. Inhibition efficiency increases with increasing the concentration and decreases slightly with an increase in temperature from 303 to 333 K. All inhibitors acted as mixed-type. Langmuir adsorption isotherm was found to be best fit among different isotherms. SEM and AFM analyses showed the formation of a protective film of the inhibitor on the AA surface.

Conflict of interest

There are no conflict of interest.

Acknowledgement

Authors are highly thankful to Prof. V. B. Singh, Head (Department of chemistry), B.H.U. for providing SEM and AFM facilities for successful completion of my research work.

References

- Abdel-Gaber, M.A., Khamis, E., Abo-EIDahab, H., Adeel, Sh., 2008. Inhibition of aluminium corrosion in alkaline solutions using natural compound. *Mater. Chem. Phys.* 109, 297–305.
- Abiola, O.K., Otaigbe, J.O.E., 2008. Effect of common water contaminants on the corrosion of aluminium alloys in ethylene glycol–water solution. *Corros. Sci.* 50, 242–247.
- Abiola, O.K., Otaigbe, J.O.E., 2009. The effect of *Phyllanthus amarus* extract on corrosion and kinetics of corrosion process of aluminium in alkaline solution. *Corros. Sci.* 51, 2790–2793.
- Abood, H.A., 2011. The study of the inhibitory properties of Omeprazole on the corrosion of Aluminium 6063 in alkaline media. *Basrah J. Sci.* 28, 74–93.
- Anejjar, A., Salghi, R., Zarrouk, A., Benali, O., Zarrok, H., Hammouti, B., Ebenso, E.E., 2014. Inhibition of carbon steel corrosion in 1 M HCl medium by potassium thiocyanate. *J. Assoc. Arab Univ. Basic Appl. Sci.* 15, 21–27.
- Ansari, K.R., Quraishi, M.A., 2015. Effect of three component (aniline–formaldehyde and piperazine) polymer on mild steel corrosion in hydrochloric acid medium. *J. Assoc. Arab Univ. Basic Appl. Sci.* 18, 12–18.
- Bammou, L., Belkhaouda, M., Salghi, R., Benali, O., Zarrouk, A., Zarrok, H., Hammouti, B., 2014. Corrosion inhibition of steel in sulfuric acidic solution by the *Chenopodium Ambrosioides* extracts. *J. Assoc. Arab Univ. Basic Appl. Sci.* 16, 83–90.
- Chaubey, N., Yadav, D.K., Singh, V.K., Quraishi, M.A., 2015. A comparative study of leaves extracts for corrosion inhibition effect on aluminium alloy in alkaline medium. *Ain Shams Eng. J.* <http://dx.doi.org/10.1016/j.asej.2015.08.020>.
- Chaubey, N., Singh, V.K., Savita, Quraishi, M.A., Ebenso, E.E., 2015. Corrosion inhibition of aluminium alloy in alkaline media by *Neolamarkia Cadamba* Bark extract as a green inhibitor. *Int. J. Electrochem. Sci.* 10, 504–518.
- Chidozie, V.N., Adoga, G.I., 2014. Potentiating effect of aqueous extract of *Anogeissus leiocarpus* on *Carica papaya* aqueous leaf extract and *Mangifera indica* aqueous stem bark extract – a herbal product used against typhoid fever in Nigeria. *Int. J. Curr. Microbiol. Appl. Sci.* 3, 1046–1062.
- Hakeem, M., Rajendran, S., Regis, A.P.P., 2014. Calcium gluconate as a corrosion inhibitor for aluminium. *JEC&AS* 3, 1–11.
- Harika, D., Swamy, A., Subhashini, V., 2013. Potential of *Terminalia arjuna* as a source of diverse drugs. *Indian j. app. res.* 3, 1–2.
- Mishra, G., Singh, P., Verma, R., Kumar, S., Srivastav, S., Jha, K.K., Khosa, R.L., 2011. Traditional uses, phytochemistry and pharmacological properties of *Moringa oleifera* plant: an overview. *Der. Pharmacia. Lettre.* 3, 141–164.
- Oguzie, E.E., 2007. Corrosion inhibition of aluminium in acidic and alkaline media by *Sansevieria trifasciata* extract. *Corros. Sci.* 49, 1527–1539.
- Prabhu, D., Rao, P., 2014. Corrosion behaviour of 6063 aluminium alloy in acidic and in alkaline media. *Arabian J. Chem.* <http://dx.doi.org/10.1016/j.arabjc.2013.07.059>.
- Quraishi, M.A., Singh, A., Singh, V.K., Yadav, D.K., Singh, A.K., 2010. Green approach to corrosion inhibition of mild steel in hydrochloric acid and sulphuric acid solutions by the extract of *Murraya koenigii* leaves. *Mater. Chem. Phys.* 122, 114–122.
- Singh, A., Ahamad, I., Quraishi, M.A., 2012. *Piper longum* extract as green corrosion inhibitor for aluminium in NaOH solution. *Doi.org/10.1016/j.arabjc.2012.04.029*.
- Yadav, D.K., Quraishi, M.A., 2012. Application of some condensed uracils as corrosion inhibitors for mild steel: gravimetric, electrochemical, surface morphological, UV–visible and theoretical investigations. *Ind. Eng. Chem. Res.* 51, 14966–14979.